Corrosion Science 54 (2012) 36–44

Contents lists available at SciVerse ScienceDirect

Corrosion Science

journal homepage: www.elsevier.com/locate/corsci

2-Butyne-1,4-diol as a novel corrosion inhibitor for API X65 steel pipeline in carbonate/bicarbonate solution

E. Sadeghi Meresht [a], T. Shahrabi Farahani [a,*], J. Neshati [b]

[a] Materials Engineering Department, Faculty of Engineering, Tarbiat Modares University, 1411713114, Tehran, Iran
[b] Research Institute of Petroleum Industry, RIPI, 1485733111, Tehran, Iran

ARTICLE INFO

Article history:
Received 26 April 2011
Accepted 28 August 2011
Available online 9 September 2011

Keywords:
A. Steel
B. Electrochemical calculation
B. EIS
B. AFM
C. Alkaline corrosion

ABSTRACT

The inhibition effects of 2-butyne-1,4-diol on the corrosion susceptibility of grade API 5L X65 steel pipeline in 2 M Na_2CO_3/1 M $NaHCO_3$ solution were studied by electrochemical techniques and weight loss measurements. The results indicated that this inhibitor was a mixed-type inhibitor, with a maximum percentage inhibition efficiency of approximately 92% in the presence of 5 mM inhibitor. Atomic force microscopy revealed that a protective film was formed on the surface of the inhibited sample. The adsorption of the inhibitor was found to conform to the Langmuir isotherm with the standard adsorption free energy of −21.08 kJ mol^{-1}.

1. Introduction

Steel pipelines play an important role in transporting gases and liquids throughout the world [1]. Corrosion is a serious problem in steel pipelines because replacing, repairing and maintaining them can be extremely expensive and time-consuming [1–5]. The water content accompanying the oil production process has been found to be a significant factor in the internal corrosion of steel pipelines because the water contains many corrosive agents such as carbon dioxide, hydrogen sulphides, organic acids and salts [6–14]. Cathodic protection reactions are the most common examples of aggressive corrosion processes in terms of external pipeline surfaces in soils [5,13,15–17]. For instance, these chemical reactions create considerable concentrations of carbonate/bicarbonate ions in the soil environment [5,18–22].

For many years, the application of corrosion inhibitors, such as organic inhibitors, has been the most common method for controlling (reducing) the corrosion of steel pipelines in acidic and alkaline environments [23–27]. In aqueous alkaline systems, the presence of certain ions such as carbonate/bicarbonate ions tends to oppose the action of inhibitors.

Corrosion protection by organic inhibitors is mostly based on modification of the metal surface through the adsorption of inhibitor molecules and the subsequent formation of a protective blocking layer [2,28–34]. These compounds are often simultaneously affected by both anodic and cathodic corrosion reactions; therefore, they are sometimes referred to as mixed-type corrosion inhibitors [28–34]. Acetylenic compounds are known as strong organic corrosion inhibitors in acid solutions [35], but less effort has been directed toward investigating these inhibitors in alkaline solutions [36,37].

In general, it has been found that in alkaline solutions, the concentration of the dissolved salts has considerable influence on the performance of inhibitors and that the concentration of the inhibitor required for protection depends on the concentration of these aggressive species [38].

Two important acetylenic alcohols are 2-butyne-1,4-diol ($C_4H_6O_2$) and propargyl alcohol (C_3H_4O), which have been examined using different techniques [33]. It is generally accepted that the triple bonds of acetylenic alcohols are an important factor in corrosion inhibition because of the p-electron interactions [39–41]. Recently, the inhibitive properties of 2-butyne-1,4-diol on mild steel in sulphuric acid solutions were investigated [33]. The results indicated that the introduction of 2-butyne-1,4-diol into sulphuric acid solution can lead to the formation of a thin inhibitor film on the steel surface, which causes a decrease in the surface roughness and effectively protects the steel from corrosion. Other studies have also revealed that inhibition efficiency increases upon increasing the inhibitor concentration. Potentiostatic curves have shown that these inhibitors act as a mixed-type inhibitor, and the inhibition efficiency of these additives increases upon increasing the size of the acetylenic chain [33,34,42].

The objective of this study was to examine the inhibition performance of the acetylenic alcohol 2-butyne-1,4-diol and its influence on the corrosion behaviour of API X65 steel pipeline in 2 M Na_2CO_3/

* Corresponding author. Tel.: +98 21 82883378; fax: +98 21 88005040.
E-mail address: tshahrabi34@modares.ac.ir (T. Shahrabi Farahani).

0010-938X/$ - see front matter © 2011 Elsevier Ltd. All rights reserved.
doi:10.1016/j.corsci.2011.08.052

1 M $NaHCO_3$ solution as well as to identify the adsorption isotherm that describes the behaviour of this inhibitor molecule on the steel pipeline surface. The effects of exposure time, inhibitor concentration and solution temperature on inhibitor performance were studied.

2. Materials and methods

2.1. Specimen

Tests were performed on a pipeline steel of the following chemical composition (wt.%): 0.07% C, 0.24% Si, 1.35% Mn, 0.017% P, 0.005% S, 0.16% Cr, 0.18% Ni, 0.12% Mo, 0.01% Cu and the remainder Fe.

This material was made according to API 5L grade X65 specifications and had a ferrite–pearlite microstructure, as shown in Fig. 1. The nominal pipe wall thickness was 1.9 mm. The yield strength of the pipe section and the ultimate tensile strength were measured to be 526 and 648 MPa, respectively, with an elongation at failure of 17%.

The specimens used in electrochemical measurements were mechanically cut into 1.0 × 1.0 × 0.5 cm dimensions, abraded by a series of emery papers (up to grade 2500) and mechanically polished to a mirror finish using aqueous alumina suspensions (with particle sizes decreasing down to 0.05 μm). Prior to each measurement, the specimen was ultrasonically cleaned for 3 min in an ethanol bath and rinsed with distilled water. Finally, the metal plate was thoroughly rinsed with distilled water.

2.2. Solution preparation

Experiments were done in stagnant 2 M Na_2CO_3/1 M $NaHCO_3$ solution in the absence and presence of different concentrations of 2-butyne-1,4-diol as a corrosion inhibitor. The molecular structure of 2-butyne-1,4-diol is shown in Fig. 2. All purchased chemicals were of reagent grade (Merck) and were used without further purification. All solutions were prepared from analytical grade reagents and distilled water. While the electrolyte solutions were in equilibrium with the atmosphere, all experiments were carried out under thermostatic conditions between 25 and 50 °C (±0.1 °C).

2.3. Weight loss measurements

Weight loss measurements were performed according to ASTM standard G 31–72 [43]. Steel specimens for each inhibitor concentration were immersed in the test solution (100 mL of 2 M Na_2CO_3/1 M $NaHCO_3$ containing various concentrations of 2-butyne-1,4-diol) in triplicate. The cleaned samples were weighed before and after immersion of the specimen into the corrosive solution and without bubbling. The submersion lasted for 3 h at a solution temperature of 25 °C, with the temperature being controlled by an aqueous thermostatted bath. The specimens were washed with distilled water and acetone, and then they were dried at room temperature. Then, an analytical balance (precision of ±0.1 mg) was used to determine the weight loss, and the mean weight loss and corresponding standard deviation were calculated.

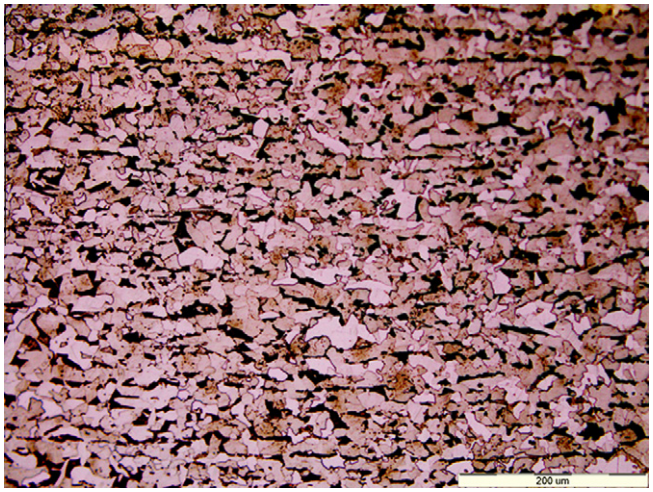

Fig. 1. Optical microstructures for API X65 steel after 5% nital etching at 25 °C.

2.4. Potentiodynamic polarization and EIS measurements

Electrochemical experiments (potentiodynamic polarization and the EIS) were performed in a conventional three-electrode cell in which a saturated calomel electrode (SCE) was the reference electrode, platinum foil was the counter electrode and the API X65 steel was the working electrode (WE). All potentials quoted in this paper were referred to the SCE. The area of the WE exposed to the solution was 0.196 cm^2.

Before electrochemical measurement the specimens were immersed in test solution at open circuit potential (E_{OCP}) for 1 h to be sufficient to attain a stable state. The polarization curve was acquired by scanning the potential range between +200 and +1400 mV (vs. OCP) using a computer-controlled potentiostat/galvanostat (EG&G Princeton Applied Research A273) at a scanning rate of 0.6 mV s^{-1}. EIS measurements were carried out using EG&G A273 with an AC amplitude of the sinusoidal perturbation of 10 mV and measurement frequency from 10 down to 100 kHz at the OCP. The computer system was equipped with a PowerSuite software analyser to record EIS data and the Zview program to determine the values of the parameters of the proposed electric circuit model. Moreover, the impedance data were fitted and the pertinent EIS parameters were extracted using the Zview program.

Fresh solution and fresh steel samples were used after each sweep. For each experimental condition, two to three measurements were performed to ensure the reliability and reproducibility of the data.

2.5. Characterization of surface films

The morphology of the corroded surface of each specimen and film formed on the steel surface were examined by Philips XL30 scanning electron microscopy. The specimens were washed and dried after being withdrawn from the test cell to enable the characterization of adherent corrosion products with no salt residues.

2.6. AFM studies

The topographic changes of the corroded surface of each specimen were monitored in standard mode with a commercial AFM Instrument from Molecular Image (Pico Scan). Micro-fabricated Si_3N_4 pyramidal cantilevers (120 μm in length) with integrated Si_3N_4 tips (20–50 nm radius of curvature) were used. The sparing constant of the cantilevers was 0.58 Nm^{-1} and the typical force during the measurements was less than 1 nm. First, the samples were abraded with SiC abrasive paper up to 4000 grade, followed by washing with distilled water and acetone. After different immersion times in 2 M Na_2CO_3/1 M $NaHCO_3$ solution with and without inhibitor at room temperature, the specimens were cleaned with distilled water and acetone, dried with a cold air blaster, and then submitted to atomic force microscopy examinations.

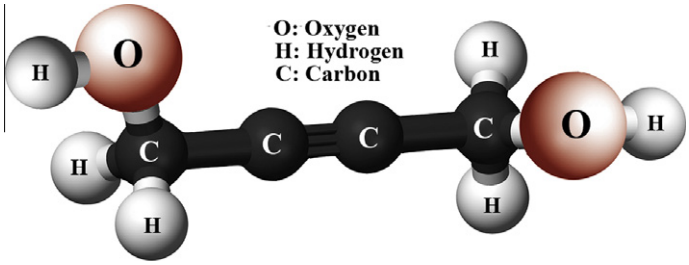

Fig. 2. Molecular structure of 2-butyne-1,4-diol.

3. Results and discussion

3.1. Weight loss measurements

The weight loss method is beneficial for monitoring inhibition efficiency because of its simple usage and reliability [44]. For the present study, the reproducibility of the weight loss and inhibition efficiency values for triplicate determinations were very accurate (±5%). Fig. 3 shows the weight loss data and the percentage inhibition efficiencies (η_w %) in 2 M Na_2CO_3/1 M $NaHCO_3$ solution at various concentrations of 2-butyne-1,4-diol and for different immersion times. The percentage inhibition efficiency (η_w %) and surface coverage (θ) were determined by the following equations:

$$\eta_w(\%) = \frac{W_0 - W_1}{W_0} \times 100 \quad (1)$$

$$\theta = \frac{W_0 - W_1}{W_0} \quad (2)$$

where $W_1$and W_0 are the values of the steel corrosion rate with and without the inhibitor, respectively. Gravimetric measurements showed that the corrosion rate decreased in the presence of 2-butyne-1,4-diol, the inhibition efficiency (η_w) increased with the 2-butyne-1,4-diol concentration and the surface coverage defined by θ reached a maximum of 0.925 at 5 mM. The inhibition can be explained by the adsorption of 2-butyne-1,4-diol [33]. Fig. 3 also shows variations of the inhibition efficiency as a function of the immersion time and concentration of the inhibitor. The inhibition increased with an increase of the immersion time and stabilised at a value of 0.925 after 3 h. Furthermore, increasing the immersion time from 3 to 6 h caused a noticeable decrease in the inhibition efficiency. This is due to the considerable inhibition efficiencies that can be realized using symmetrical acetylenic compounds. The adsorption coverage of inhibitor on the steel surface increases with the inhibitor concentration.

3.2. Potentiodynamic measurements

The potentiodynamic polarization parameters in 2 M Na_2CO_3/1 M $NaHCO_3$ solution with and without various concentrations of 2-butyne-1,4-diol at 25 °C are listed in Table 1. These parameters include the values of corrosion current densities (I_{corr}), corrosion potential (E_{corr}), cathodic Tafel slope (b_c), anodic Tafel slope (b_a) and inhibition efficiency (η_p). Both cathodic and anodic reactions were suppressed by the addition of 2-butyne-1,4-diol (Fig. 4), which suggests that 2-butyne-1,4-diol reduces anodic dissolution and retards the hydrogen evolution reaction. In other words, the presence of 2-butyne-1,4-diol causes a prominent decrease in the corrosion rate, i.e., shifts both the anodic and cathodic curves to lower current densities. Moreover, both the cathodic and anodic reactions of steel corrosion were drastically retarded by 2-butyne-1,4-diol in 2 M Na_2CO_3/1 M $NaHCO_3$. Clearly, I_{corr} was remarkably decreased, while η_p increased with the inhibitor concentration and the maximum η_p was 0.92 at 5 mM 2-butyne-1,4-diol. There was no definite trend in the shift of E_{corr} in the presence of 2-butyne-1,4-diol; therefore, 2-butyne-1,4-diol could be a mixed-type inhibitor, with the inhibitory action caused by a geometric blocking effect [44]. In addition, the inhibitory action was

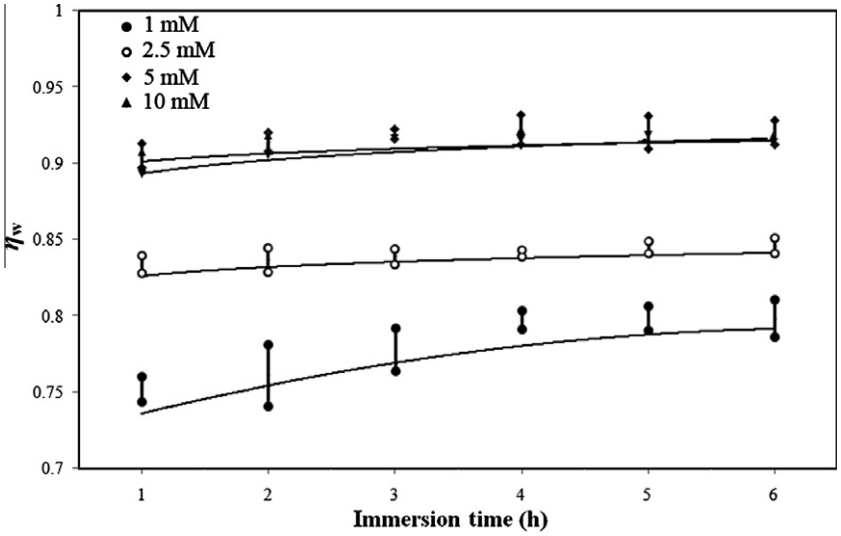

Fig. 3. Percentage inhibition efficiencies (η_w) obtained from weight loss measurements in 2 M Na_2CO_3/1 M $NaHCO_3$ solution containing different concentrations of 2-butyne-1,4-diol for different immersion times at 25 °C.

Table 1
Potentiodynamic polarization parameters for the corrosion of steel pipeline samples in 2 M Na_2CO_3/1 M $NaHCO_3$ containing different concentrations of 2-butyne-1,4-diol at 25 °C.

Concentration of inhibitor (mM)	I_{corr} (μA cm^{-2})	E_{corr} (mV vs. SCE)	b_c (mV dec^{-1})	b_a (mV dec^{-1})	Corrosion rate (mg cm^{-2} day^{-1})	η_p
Blank	3.686	−330	317	569	1.447	–
1.0	0.995	−305	142	341	0.389	0.73
2.5	0.516	−289	133	369	0.203	0.86
5.0	0.295	−276	109	261	0.116	0.92
10.0	0.332	−264	82	195	0.130	0.91

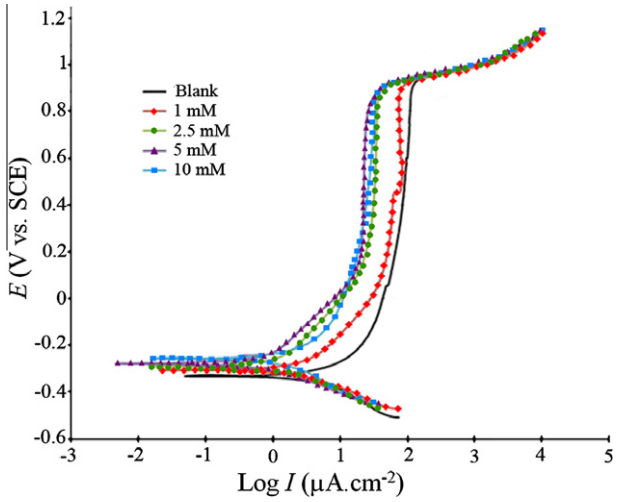

Fig. 4. Potentiodynamic polarization curves for the steel samples in 2 M Na_2CO_3/1 M $NaHCO_3$ solution containing different concentrations of 2-butyne-1,4-diol at 25 °C (the immersion time was 3 h).

due to a reduction of the reaction area on the surface of the corroding metal [45]. The inhibition efficiency (η_p) was calculated by the following equations:

$$\eta_p = \frac{I_{corr(0)} - I_{corr(inh)}}{I_{corr(0)}} \quad (3)$$

where $I_{corr(0)}$ and $I_{corr(inh)}$ are the corrosion current densities without and with the inhibitor, respectively. The anodic and cathodic Tafel slopes significantly changed in the presence of 2-butyne-1,4-diol, which may have been due to carbonate ions or inhibitor molecules adsorbed on the steel surface (Fig. 4). The behaviour indicated that 2-butyne-1,4-diol acts as a mixed-type inhibitor, affecting both the anodic and cathodic reaction mechanisms. For 2-butyne-1,4-diol, not only the Tafel slope, but also the corrosion potential was considerably changed when compared with that of the blank. It was evident from Table 1 that upon increasing the inhibitor concentration to 5 mM, corrosion current density values significantly decreased and the inhibition efficiency increased; however, a further increase in inhibitor concentration to 10 mM decreased the inhibition efficiency. This is likely because adsorptive and protective films of the inhibitor molecules were formed on the steel surface. The film acted as a physical barrier to restrict the diffusion of corrosive species to the steel surface. Additionally, the anodic slope increased, which may have been due to the formation of a protective surface film. It is worth noting that this effect is dependent on the surface conditions. When the specimens were pre-corroded, the anodic slopes were higher than when non-pre-corroded specimens were immersed in an inhibitor solution. This could be related to interactions between the corrosion products, inhibitor adsorption and film formation. Changes in the cathodic slopes were also correlated to the surface conditions. Thus, it seems that longer periods of pre-corrosion testing are required to fully understand the behaviour [46].

For 2-butyne-1,4-diol, the corrosion current density decreased and the inhibition efficiency increased upon increasing the inhibitor concentration. The highest inhibition efficiency was 0.92 at 5 mM. The inhibition efficiency increased with an increase in the surface coverage (θ). The high inhibition efficiency was due to bonding of the adsorbed film on the steel surface [24]. The inhibition efficiencies were in good agreement with those calculated from the weight loss measurements.

3.3. Electrochemical impedance spectroscopy

3.3.1. Effect of the inhibitor concentration on inhibitor performance

Fig. 5 presents Nyquist diagrams of the steel measured in 2 M Na_2CO_3/1 M $NaHCO_3$ with and without various concentrations of the inhibitor during an immersion time of 3 h at 25 °C. It should be noted that if the adsorption of inhibitors had a considerable influence on the interface, both the ratio of time constants and characterization of the adsorption process must change. The Nyquist plots consisted of two capacitive loops. The one at high frequency (in the right part of the figure) was related to charge transfer resistance, which could correlate to resistance between the steel and outer helmholtz plane [47]. Conversely, the one at low frequency (in the left part of the figure) was attributed to the adsorbed film resistance due to adsorption of the inhibitor and all other accumulated products [47]. Deviations from a perfect circular shape (depression) are often related to the frequency dispersion of interfacial impedance arising from a lack of homogeneity of the electrode surface due to roughness or interfacial phenomena [48].

The EIS results were simulated using the equivalent circuit shown in Fig. 6 in relation to pure electric models, which can verify

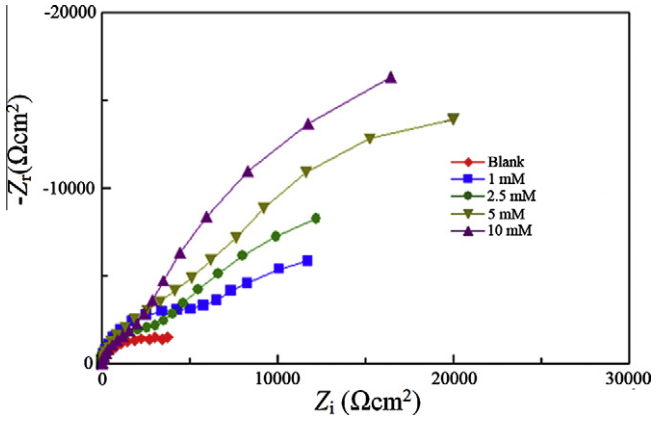

Fig. 5. Nyquist plots of the corrosion of steel in 2 M Na_2CO_3/1 M $NaHCO_3$ containing different concentrations of 2-butyne-1,4-diol at 25 °C (the immersion time was 3 h).

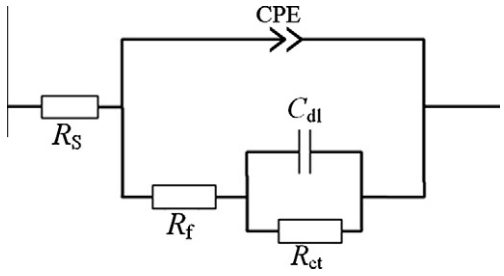

Fig. 6. Equivalent circuit used to fit the metal/acid interface containing different concentrations of 2-butyne-1,4-diol.

or rule out mechanistic models and enable the calculation of numerical values corresponding to the physical and/or chemical properties of the electrochemical system under investigation [49]. The employed circuit allowed for the identification of solution resistance (R_s), charge transfer resistance (R_{ct}) and resistance associated with the layer of products formed (R_f). It is worthy of note that the double layer capacitance (C_{dl}) value was affected by imperfections of the surface, and this effect was simulated via a constant phase element (CPE) [50]. The constant phase element was composed of the component Q_{dl} and coefficient n. The parameter n quantifies different physical phenomena, such as surface heterogeneousness resulting from surface roughness, inhibitor adsorption and porous layer formation. Therefore, the capacitance was deduced by the following equations [51]:

$$CPE = Q_{dl} \times (2\pi f_{max})^{n-1} \quad (4)$$

where f_{max} represents the frequency at which the imaginary value reaches a maximum on the Nyquist plot. According to the above-mentioned equivalent circuits, the experimental data were fitted very well and the impedance diagrams for 2-butyne-1,4-diol could be described well using the model presented in Fig. 6. The percentage inhibition efficiency was calculated by the following equations:

$$\eta(\%) = \frac{R_{ct(0)} - R_{ct(inh)}}{R_{ct(0)}} \times 100 \quad (5)$$

where $R_{ct(0)}$ and $R_{ct(inh)}$ are values of the charge transfer resistance observed in the absence and presence of 2-butyne-1,4-diol. The EIS parameters are also summarized in Table 2. The electrochemical parameters of R_{ct}, C_{dl} and η were calculated with the Zview software and are presented in Table 2. Based on Table 2, the R_{ct} values were prominently increased while the C_{dl} values declined with the concentration of 2-butyne-1,4-diol. Theoretically, the decrease in C_{dl} was comparable to that in the blank solution, which can result from a decrease in local dielectric constant and/or an increase in the thickness of the electrical double layer, suggesting that inhibitor molecules function through adsorption at the metal/solution interface [24]. The impedance spectra consisted of small capacitive loops at high frequencies followed by a large loop at low frequency values. The high frequency capacitive loop was related to charge transfer of the corrosion process and the double layer behaviour. In addition, the low frequency inductive loop may have been due to the relaxation process of adsorbed species, such as inhibitor species [52], on the electrode surface. It may also have been due to re-dissolution of the passivated surface at low frequencies [52]. These high frequency loops were not perfect semicircles, which could be attributed to frequency dispersion because of the roughness and heterogeneousness of the electrode surface [53]. Furthermore, the diameter of the capacitive loop in the presence of inhibitor increased with the inhibitor concentration and was larger than that in the absence of inhibitor (blank solution). This behaviour indicated that impedance of the inhibited substrate increased upon increasing the inhibitor concentration. Table 2 shows that the capacitance values decreased and the charge transfer resistance increased upon increasing the inhibitor concentration, and the obtained η values were in good agreement with those determined from the polarization curves.

The inhibition efficiency increased with the concentration of 2-butyne-1,4-diol and the maximum inhibition efficiency was 0.924, which further confirmed that 2-butyne-1,4-diol exhibits very good inhibitive performance for steel in 2 M Na_2CO_3/1 M $NaHCO_3$. The inhibition efficiencies obtained from weight loss measurements (η_w), potentiodynamic polarization curves (η_p) and EIS (η) were in reasonable agreement. A comparison of the η values (Table 3) obtained using these three methods also showed acceptable agreement. This agreement among three independent techniques proves the validity of the results.

3.3.2. The effects of immersion time on the inhibitor performance

To investigate the 2-butyne-1,4-diol adsorption kinetics and determine the time needed for 2-butyne-1,4-diol to reach its maximum inhibition efficiency, EIS experiments were carried out in the presence of 5 mM 2-butyne-1,4-diol in 2 M Na_2CO_3/1 M $NaHCO_3$ at different immersion times at 25 °C (Fig. 7). A comparison of the results of R_{ct} with 5 mM 2-butyne-1,4-diol at different immersion times is presented in Table 4. R_{ct} increased upon increasing the immersion time up to 3 h and then became relatively constant. From the figure, R_{ct} slightly increased upon increasing the inhibitor concentration at a given immersion time. This may indicate that the inhibitor film becomes slightly more effective at higher inhibitor concentrations. Increasing the inhibitor concentration may not yield good performance of the inhibitor film for longer immersion times. The decrease in C_{dl} values was caused by an imperceptible replacement of water molecules due to the adsorption of inhibitor molecules on the steel surface, decreasing the extent of the dissolution reaction [54,55]. The corresponding corrosion resistance and corrosion inhibition efficiency values were calculated and are presented in Table 4. The data demonstrated that even 3 h after adding 2-butyne-1,4-diol to the electrolyte, the corrosion inhibition efficiency reached 0.924. The AC impedance study also corroborated the inhibitory character of 2-butyne-1,4-diol obtained based on polarization curves. Inhibitors usually act at a solid surface by forming an adsorbed film or by inducing the formation a layer of corrosion products. The adsorption depends on the charge of the metallic surface, the charge or dipole moment of the inhibitor molecule and the adsorption of other ionic species present in solution [56].

3.3.3. The effects of solution temperature on inhibitor performance

The influence of temperature on the corrosion inhibition efficiency of 2-butyne-1,4-diol was studied in a temperature interval

Table 2
EIS parameters obtained from the corrosion of steel 2 M Na_2CO_3/1 M $NaHCO_3$ containing different concentrations of 2-butyne-1,4-diol at 25 °C (the immersion time was 3 h).

Concentration of the inhibitor (mM)	C_{dl} (μF cm^{-2})	R_s (Ω cm^2)	R_P (Ω cm^2)	CPE (μF cm^{-2})	n	R_{ct} (Ω cm^2)	η
Blank	5092	5.559	23.79	934	0.85	38	–
1.0	1476	5.223	82.03	270	0.86	131	0.710
2.5	814	5.374	148.70	150	0.87	237	0.840
5.0	387	5.608	313.01	71	0.87	500	0.924
10.0	509	4.228	237.90	93	0.88	380	0.900

Table 3
Inhibition efficiency values obtained from weight loss, potentiodynamic polarization and electrochemical impedance measurements of steel in 2 M Na_2CO_3/1 M $NaHCO_3$ solution containing various concentrations of 2-butyne-1,4-diol at 25 °C (the immersion time was 3 h).

Concentration of the inhibitor (mM)	Inhibition efficiency		
	Weight loss	Potentiodynamic polarization	EIS
1.0	0.796	0.730	0.710
2.5	0.841	0.860	0.840
5.0	0.925	0.920	0.924
10.0	0.921	0.910	0.900

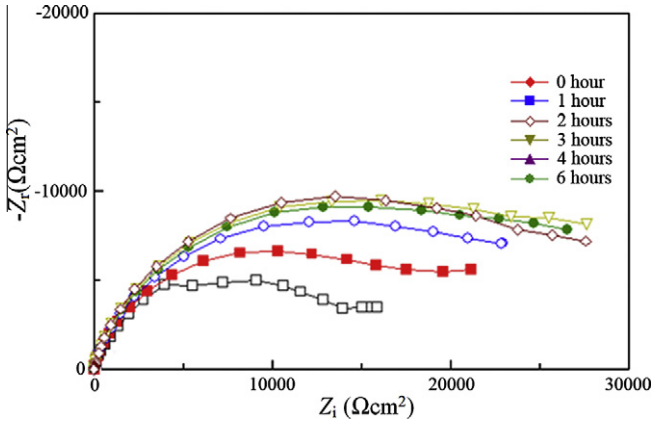

Fig. 7. Nyquist plots of the corrosion of steel in 2 M Na_2CO_3/1 M $NaHCO_3$ solution at different immersion times at 25 °C (the concentration of 2-butyne-1,4-diol was 5 mM).

from 25 to 50 °C in 2 M Na_2CO_3/1 M $NaHCO_3$ solution. Fig. 8 shows the corresponding results of the corrosion inhibition efficiency calculated using EIS measurements. It was found that with increasing temperature, the steel corrosion resistance decreased in both the presence and absence of 2-butyne-1,4-diol, which was expected. However, the decreasing trend in the corresponding corrosion inhibition efficiency (Table 5) indicated that the relative steel corrosion resistance in the presence of 2-butyne-1,4-diol was more temperature-dependent than that in the absence of 2-butyne-1,4-diol. This could be explained on the basis of temperature-dependent 2-butyne-1,4-diol adsorption/desorption processes. For example, with an increase in temperature, the 2-butyne-1,4-diol adsorption equilibrium could shift towards the desorption process, resulting in a lower surface coverage [37]. This would also result in a decrease in 2-butyne-1,4-diol surface conformation order and, thus, decrease the protection against corrosive ions. Nevertheless, the corrosion inhibition efficiency was relatively high, even at 50 °C. Noor et al. [57] suggested that with an increase in temperature, some chemical changes occur in the inhibitor molecules, leading to an increase in the electron density at the adsorption centres of the molecule, which causes an improvement in inhibition efficiency.

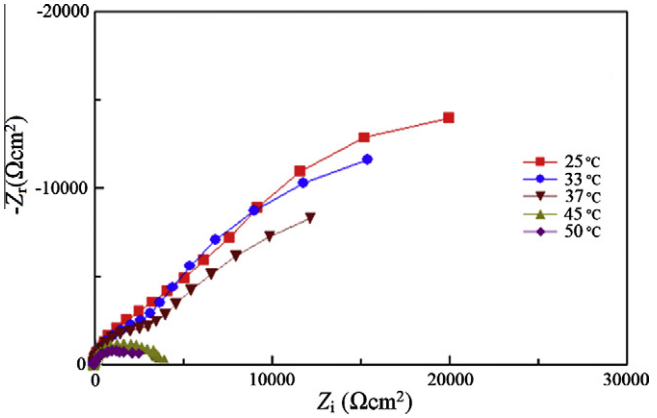

Fig. 8. Nyquist plots of the corrosion of steel in 2 M Na_2CO_3/ 1 M $NaHCO_3$ solution at different temperatures (the concentration of 2-butyne-1,4-diol was 5 mM and the immersion time was 3 h).

3.4. Adsorption isotherm

Generally, the essential step in an inhibition mechanism is the adsorption of inhibitors on the steel surface [58]; therefore, the increase in corrosion inhibition is caused by the adsorption of inhibitors on the steel surface. To describe the adsorption of 2-butyne-1,4-diol on the steel surface, several adsorption isotherms were tested, including Freundlich, Temkin, Frumkin, Bockris–Swinkels, Flory–Huggins and Langmuir isotherms. However, the best agreement was obtained using the Langmuir adsorption isothermal equation as follows:

$$\frac{\theta}{1-\theta} = K_{ads}.c \tag{6}$$

where c is the concentration of the inhibitor, K_{ads} is the adsorptive equilibrium constant and θ is the degree of surface coverage of the inhibitor molecule, which is given by the following equation:

$$\theta = \frac{R_{ct(0)} - R_{ct(inh)}}{R_{ct(0)}} \tag{7}$$

where $R_{ct(0)}$ and $R_{ct(inh)}$ are the charge transfer resistance in the absence and presence of inhibitors, respectively. Consequently, if the Langmuir isotherm describes the inhibitor adsorption process, a plot of experimental data expressed as (c/θ) vs. (c) should yield a straight line with a linear correlation coefficient (r) and slope very close to unity. For both the EIS and weight loss experiments and the Langmuir isotherm data, the agreement was very good ($r^2 = 0.999$), which indicated an excellent inhibition of steel corrosion through the adsorption of 2-butyne-1,4-diol on the steel surface. The superiority of this process was also confirmed by the good agreement between the values obtained from the polarization and impedance studies and weight loss measurements.

However, the width of the original value of the (c/θ) versus (c) plots showed little deviation from zero, which signified non-ideal and unexpected deviations from the Langmuir adsorption isotherm.

Table 4
EIS parameters obtained from the corrosion of steel 2 M Na_2CO_3/1 M $NaHCO_3$ solution for different immersion times at 25 °C (the concentration of 2-butyne-1,4-diol was 5 mM).

Immersion time (h)	C_{dl} (μF cm^{-2})	R_s (Ω cm^2)	R_P (Ω cm^2)	CPE (μF cm^{-2})	n	R_{ct} (Ω cm^2)	η
0	5160	5.968	22.72	402	0.85	38.0	–
1	820	5.876	144.16	96	0.85	237.5	0.840
2	675	3.951	182.76	73	0.86	292.3	0.870
3	387	5.607	313.01	71	0.87	500.0	0.924
4	402	5.419	296.84	109	0.87	493.5	0.923
6	381	5.409	303.55	115	0.88	506.7	0.925

Table 5
EIS parameters obtained from the corrosion of steel 2 M Na_2CO_3/1 M $NaHCO_3$ solution at different temperatures (the concentration of 2-butyne-1,4-diol is 5 mM and the immersion time was 3 h).

T (°C)	C_{dl} (μF cm^{-2})	R_s (Ω cm^2)	R_P (Ω cm^2)	CPE (μF cm^{-2})	n	R_{ct} (Ω cm^2)
25	387.00	5.607	313.01	71	0.87	500.0
32	486.73	5.530	172.57	107	0.86	441.6
40	678.58	5.355	48.67	113	0.87	315.8
45	1071.42	4.020	27.83	121	0.86	21.9
50	2653.06	3.357	17.97	152	0.84	21.3

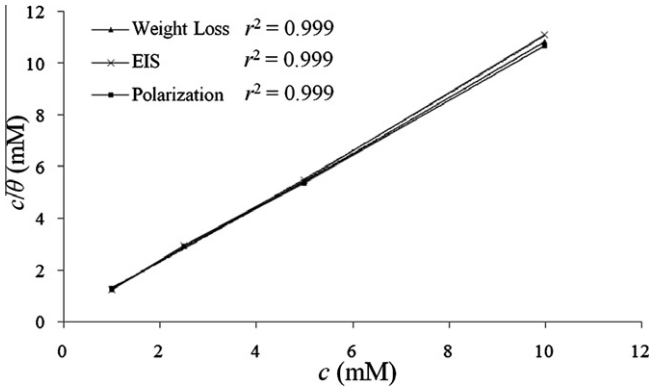

Fig. 9. Langmuir isotherm adsorption model of 2-butyne-1,4-diol on the surface of steel in 2 M Na_2CO_3/1 M $NaHCO_3$ solution.

This could be due to interactions between the adsorbed species on the steel surface [59,60]. With respect to the weight loss results in Fig. 9, the calculated adsorptive equilibrium constant (K_{ads}) value was 5000 M^{-1} and the standard adsorption free energy (ΔG^0) was calculated by the following equations [61]:

$$\Delta G^{\circ} = RTlnK_{ads} \quad (8)$$

where R is the gas constant (8.314 J K^{-1} mol^{-1}) and T is the absolute temperature(K). The calculated ΔG^0 value was −21.08 kJ mol^{-1}. Generally, values of ΔG^0 up to −20 kJ mol^{-1} indicate adsorption with electrostatic interaction between the adsorbent and adsorbate (physisorption) and the charged metal (physical adsorption), while negative values of more than −40 kJ mol^{-1} involve the sharing or transfer of electrons from inhibitor molecules to the steel surface to form a coordinate type of bond (chemisorption) [31]. In the present study, the value of ΔG^0 was slightly more negative than −20 kJ mol^{-1}, likely indicating that the adsorption mechanism of the 2-butyne-1,4-diol on steel in 2 M Na_2CO_3/1 M $NaHCO_3$ solution was mainly chemisorption. In fact, the role of non-paired electrons of oxygen atoms and the triple bond in acetylenic alcohol molecules cannot be ignored. In other words, in this case, acetylene alcohol forms a film whose strength on the steel surface is due to hydrogen and π bonding. Initial absorption likely takes place through the π triple bond, while hydroxyl groups reinforce the triple bond by giving electrons to the steel surface. According to studies on the corrosion inhibition of 2-butyne-1,4-diol, the inhibition mechanisms could include both physical absorption and absorption through the sharing of electrons with the steel surface.

The K_{ads} values showed the strength of the adsorption forces between the inhibitor molecules and steel surface. According to the values obtained for K_{ads}, the interaction between the double layer that exists in the phase boundary and the adsorbed molecules appeared to be relatively strong.

3.5. Surface morphology

The corrosion efficiency of 2-butyne-1,4-diol on steel in 2 M Na_2CO_3/1 M $NaHCO_3$ was also clearly visible in Fig. 10, which shows the steel surface topography in the testing electrolyte in the absence and presence of the inhibitor. Fig. 10a shows the steel surface in the solution before immersion. Fig. 10b demonstrates that in the absence of the inhibitor, surface corrosion was extensive and could clearly be seen in the form of significant surface damage. The figure confirmed the presence of uneven corrosion products arranged layer upon layer and in rough surface layers. In contrast, in the presence of 5 mM 2-butyne-1,4-diol (Fig. 10c), the steel surface was corroded only negligibly. In addition, there was an adsorbed film on the steel surface that was not observed in Fig. 10a. The result was an enhancement of surface coverage on the steel surface such that there was a decrease in contact between the steel and the aggressive medium. Thus, a good absorptive protection layer can efficiently inhibit the corrosion of steel.

3.6. AFM studies

The surface microstructure of the steel in 2 M Na_2CO_3/1 M $NaHCO_3$ solution before and after immersion and in the presence of 5 mM 2-butyne-1,4-diol after 3 h of immersion time was investigated using AFM (Fig 11). The corroded surface in 2 M Na_2CO_3/1 M $NaHCO_3$ solution in the absence of 2-butyne-1,4-diol looked relatively uneven and appeared to have potholes, while it was relatively flat and compact in the presence of 5 mM 2-butyne-1,4-diol (Fig. 11(a)–(c)). It is clearly shown in Fig. 11(c) that the uncorroded

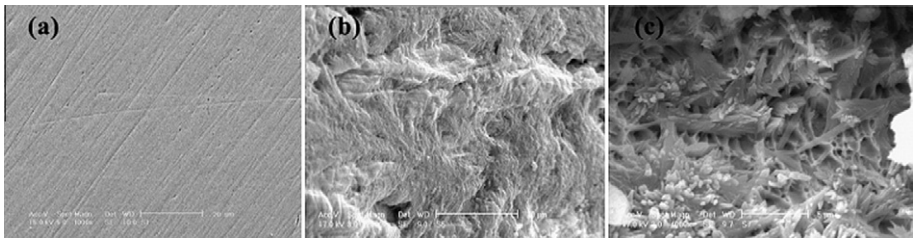

Fig. 10. (a) SEM image of steel surface taken after immersion in 2 M Na_2CO_3/1 M $NaHCO_3$ solution, (b) SEM image of steel surface taken after immersion in 2 M Na_2CO_3/1 M $NaHCO_3$ solution in the absence of 2-butyne-1,4-diol, (c) SEM image of steel surface taken after immersion in 2 M Na_2CO_3/1 M $NaHCO_3$ solution in the presence of 5 mM of 2-butyne-1,4-diol.

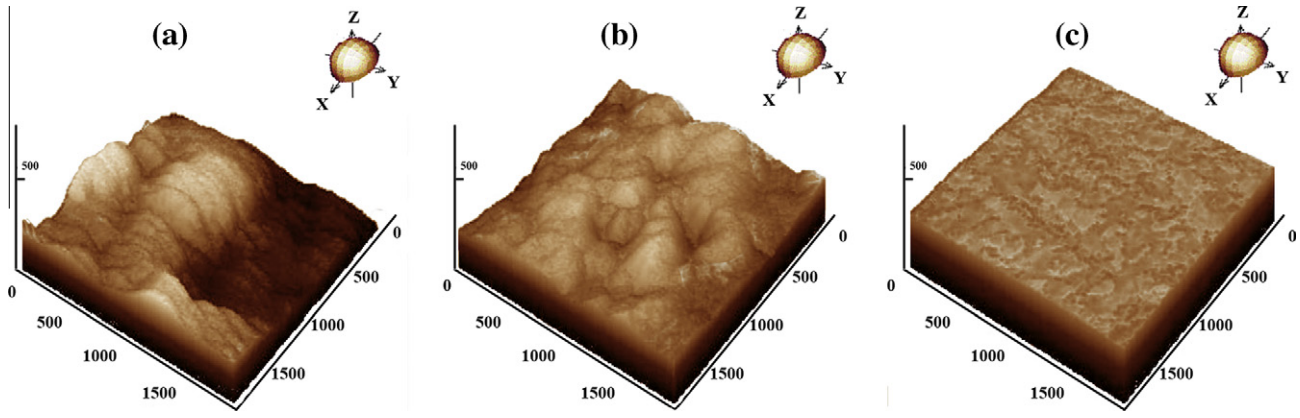

Fig. 11. Atomic force microscopy three-dimensional images of steel surface in 2 M Na_2CO_3/1 M $NaHCO_3$ solution (a) without inhibitor, (b) containing 5 mM 2-butyne-1,4-diol after immersion in 2 M Na_2CO_3/1 M $NaHCO_3$ solution at 25 °C and (c) containing 5 mM 2-butyne-1,4-diol at 25 °C (the immersion time was 3 h).

surface in the presence of the inhibitor was more uniform than the corroded one in the absence of inhibitor. The uneven and potholed steel in Na_2CO_3/$NaHCO_3$ solution without 2-butyne-1,4-diol indicated that steel the corrosion in this solution was typically electrochemical corrosion, while the more even surface in the presence of 2-butyne-1,4-diol suggested that 2-butyne-1,4-diol in Na_2CO_3/$NaHCO_3$ solution can form an inhibitive film on the steel surface that protects it from corrosion. An analysis of the data in Fig. 11 showed that the layer height values were about 300 and 400 nm, respectively. Thus, the corrosion of steel decreases after adding 2-butyne-1,4-diol to 2 M Na_2CO_3/1 M $NaHCO_3$ solution. In the presence of 2-butyne-1,4-diol, the surface porosity and corrosion rate were lower than those in the absence of 2-butyne-1,4-diol. This was due to the adsorption of the 2-butyne-1,4-diol on the surface, so the roughness of surface was very low. A comparison of Fig. 11a, b and c clearly shows that the corrosion of steel decreased in the presence of 2-butyne-1,4-diol.

4. Conclusions

In this study, the inhibition efficiency of 2-butyne-1,4-diol on steel in 2 M Na_2CO_3/1 M $NaHCO_3$ solution was determined by weight loss and electrochemical techniques such as polarization and impedance measurements. The inhibition efficiency increased upon increasing of the inhibitor concentration; however, it decreased upon increasing the temperature. The adsorption of 2-butyne-1,4-diol on the steel obeyed the Langmuir adsorption isotherm model. Its inhibition action was due to the physical adsorption of 2-butyne-1,4-diol on the surface of the steel. A mixed inhibition mechanism was proposed for the inhibitive effects of 2-butyne-1,4-diol based on the polarization results. The introduction of 2-butyne-1, 4-diol into 2 M Na_2CO_3/1 M $NaHCO_3$ solution resulted in the formation of a thin inhibitor film on the steel surface, causing a decrease in surface roughness and effectively protecting the steel from corrosion. The equivalent circuit was selected based on properties of the EIS Nyquist diagrams and fit the experimental data well. The inhibition efficiencies were determined by polarization and EIS plots, which were in good agreement with the weight loss measurements. The changes in the impedance parameters confirmed the strong adsorption of the inhibitor on the steel surface, which prevented anodic dissolution of the metal by blocking active metal surface sites. Furthermore, in the presence of the inhibitor, the double layer capacitance decreased, which confirmed adsorption of the inhibitor molecules on the steel surface. The SEM results showed the formation of a protective and dense layer on the steel surface in the presence of the inhibitor.

References

[1] S. Ghareba, S. Omanovic, Interaction of 12-aminododecanoic acid with a carbon steel surface. Towards the development of 'green' corrosion inhibitors, Corrosion Science 52 (2010) 2104–2113.
[2] M.A. Hegazy, M. Abdallah, H. Ahmed, Novel cationic gemini surfactants as corrosion inhibitors for carbon steel pipelines, Corrosion Science 52 (2010) 2897–2904.
[3] A. Hernández-Espejel, M.A. Domínguez-Crespo, R. Cabrera-Sierra, C. Rodríguez-Meneses, E.M. Arce-Estrada, Investigations of corrosion films formed on API-X52 pipeline steel in acid sour media, Corrosion Science 52 (2010) 2258–2267.
[4] M.A. Hegazy, H.M. Ahmed, A.S. El-Tabei, Investigation of the inhibitive effect of p-substituted 4- (*N*, *N*, *N*-dimethyldodecylammonium bromide) benzylidene-benzene-2-yl-amine on corrosion of carbon steel pipelines in acidic medium, Corrosion Science 53 (2011) 671–678.
[5] E. Sadeghi Meresht, T. Shahrabi Farahani, J. Neshati, Failure analysis of stress corrosion cracking occurred in a gas transmission steel pipeline, Engineering Failure Analysis 18 (2011) 963–970.
[6] M.A. Migahed, Corrosion inhibition of steel pipelines in oil fields by N, N-di(poly oxy ethylene) amino propyl lauryl amide, Progress in Organic Coatings 54 (2005) 91–98.
[7] S. Nešić, Key issues related to modelling of internal corrosion of oil and gas pipelines – A review, Corrosion Science 49 (2007) 4308–4338.
[8] J.W. Graves, E.H. Sullivan, Internal corrosion in gas gathering system and transmission lines, Material Protection 5 (1996) 33–37.
[9] N. Muthukumar, S. Maruthamuthu, N. Palaniswamy, Water-soluble inhibitor on microbiologically influenced corrosion in diesel pipeline, Colloids and Surfaces B: Biointerfaces 53 (2006) 260–270.
[10] A. Rajasekar, T. Ganesh Babu, S. Karutha Pandian, S. Maruthamuthu, N. Palaniswamy, A. Rajendran, Biodegradation and corrosion behavior of manganese oxidizer Bacillus cereus ACE4 in diesel transporting pipeline, Corrosion Science 49 (2007) 2694–2710.
[11] X. Jiang, Y.G. Zheng, W. Ke, Effect of flow velocity and entrained sand on inhibition performances of two inhibitors for CO_2 corrosion of N80 steel in 3% NaCl solution, Corrosion Science 47 (2005) 2636–2658.
[12] F.G. Liua, M. Du, J. Zhanga, M. Qiua, Electrochemical behavior of Q235 steel in saltwater saturated with carbon dioxide based on new imidazoline derivative inhibitor, Corrosion Science 51 (2009) 102–109.
[13] D. Hardie, E.A. Charles, A.H. Lopez, Hydrogen embrittlement of high strength pipeline steels, Corrosion Science 48 (2006) 4378–4385.
[14] Y.F. Cheng, Analysis of electrochemical hydrogen permeation through X-65 pipeline steel and its implications on pipeline stress corrosion cracking, International Journal of Hydrogen Energy 32 (2007) 1269–1276.
[15] G.K. Glass, J.R. Chadwick, An investigation into the mechanisms of protection afforded by a cathodic current and the implications for advances in the field of cathodic protection, Corrosion Science 36 (1994) 2193–2209.
[16] X. Chen, X.G. Li, C.W. Du, Y.F. Cheng, Effect of cathodic protection on corrosion of pipeline steel under disbonded coating, Corrosion Science 51 (2009) 2242–2245.
[17] M.T. Lilly, S.C. Ihekwoaba, S.O.T. Ogaji, S.D. Probert, Prolonging the lives of buried crude-oil and natural-gas pipelines by cathodic protection, Applied Energy 84 (2007) 958–970.
[18] B.T. Lu, F. Song, M. Gao, M. Elboujdaini, Crack growth model for pipelines exposed to concentrated carbonate–bicarbonate solution with high pH, Corrosion Science 52 (2010) 4064–4072.

[19] G.A. Zhang, Y.F. Cheng, On the fundamentals of electrochemical corrosion of X65 steel in CO_2-containing formation water in the presence of acetic acid in petroleum production, Corrosion Science 51 (2009) 87–94.
[20] M.C. Li, Y.F. Cheng, Corrosion of the stressed pipe steel in carbonate–bicarbonate solution studied by scanning localized electrochemical impedance spectroscopy, Electrochimica Acta 53 (2008) 2831–2836.
[21] A. Torres-Islas, V.M. Salinas-Bravo, J.L. Albarran, J.G. Gonzalez-Rodriguez, Effect of hydrogen on the mechanical properties of X-70 pipeline steel in diluted $NaHCO_3$ solutions at different heat treatments, International Journal of Hydrogen Energy 30 (2005) 1317–1322.
[22] D.G. Li, Y.R. Feng, Z.Q. Bai, J.W. Zhu, M.S. Zheng, Influence of temperature, chloride ions and chromium element on the electronic property of passive film formed on carbon steel in bicarbonate/carbonate buffer solution, Electrochimica Acta 52 (2007) 7877–7884.
[23] H. Ju, Y. Li, Nicotinic acid as a nontoxic corrosion inhibitor for hot dipped Zn and Zn–Al alloy coatings on steels in diluted hydrochloric acid, Corrosion Science 49 (2007) 4185–4201.
[24] V.R. Saliyan, A.V. Adhikari, Quinolin-5-ylmethylene-3-{[8-(trifluoromethyl) quinolin-4-yl]thio} propanohydrazide as an effective inhibitor of mild steel corrosion in HCl solution, Corrosion Science 50 (2008) 55–61.
[25] C. Kustu, K.C. Emregul, O. Atakol, Schiff bases of increasing complexity as mild steel corrosion inhibitors in 2 M HCl, Corrosion Science 49 (2007) 2800–2814.
[26] P. Galicia, I. González, Modification of 1018 carbon steel corrosion process in alkaline sour medium with a formulation of chemical corrosion inhibitors, Electrochem Acta 50 (2005) 4451–4460.
[27] M.B. Valcarce, M. Vázquez, Carbon steel passivity examined in alkaline solutions: The effect of chloride and nitrite ions, Electrochem Acta 53 (2008) 5007–5015.
[28] A. Popova, M. Christov, S. Raicheva, E. Sokolova, Adsorption and inhibitive properties of benzimidazole derivatives in acid mild steel corrosion, Corrosion Science 46 (2004) 1333–1350.
[29] A. Döner, R. Solmaz, M. Özcan, G. Kardaş, Experimental and theoretical studies of thiazoles as corrosion inhibitors for mild steel in sulphuric acid solution, Corrosion Science 53 (2011) 2902–2913.
[30] D. Zhang, Zh. An, Q. Pan, L. Gao, G. Zhou, Comparative study of bis-piperidiniummethyl-urea and mono-piperidiniummethyl-urea as volatile corrosion inhibitors for mild steel, Corrosion Science 48 (2006) 1437–1448.
[31] F. Bentiss, M. Lebrini, M. Lagrenée, Thermodynamic characterization of metal dissolution and inhibitor adsorption processes in mild steel/2, 5-bis(*n*-thienyl)-1, 3, 4-thiadiazoles/hydrochloric acid system, Corrosion Science 47 (2005) 2915–2931.
[32] E.E. Oguziea, Y. Lia, F.H. Wang, Corrosion inhibition and adsorption behaviour of methionine on mild steel in sulphuric acid and synergistic effect of iodide ion, Journal of Colloid and Interface Science 310 (2007) 90–98.
[33] M.G. Hosseini, M.R. Arshadi, Study of 2-butyne-1, 4-diol as Acid Corrosion Inhibitor for Mild Steel with Electrochemical, infrared and AFM Techniques, International journal of Electrochemical Science 4 (2009) 1339–1350.
[34] G. Gece, The use of quantum chemical methods in corrosion inhibitor studies, Corrosion Science 50 (2008) 2981–2992.
[35] J.O'M. Bockris, Bo Yang, The Mechanism of Corrosion Inhibition of Iron in Acid Solution by Acetylenic Alcohols, journal of the electrochemical society 138 (1991) 2237–2252.
[36] A. Popova, M. Christov, A. Zwetanova, Effect of the molecular structure on the inhibitor properties of azoles on mild steel corrosion in 1 M hydrochloric acid, Corrosion Science 49 (2007) 2131–2143.
[37] A. Popova, M. Christov, A. Vasilev, Inhibitive properties of quaternary ammonium bromides of *N*-containing heterocycles on acid mild steel corrosion, Part II: EIS results, Corrosion Science 49 (2007) 3290–3302.
[38] M.A. Ameer, A.M. Fekry, Corrosion inhibition of mild steel in acidic media using newly synthesized heterocyclic organic molecules, International Journal of Hydrogen Energy 35 (2010) 11387–11396.
[39] M.G. Veliev, N.M. Agaev, M.I. Shatirova, A.Z. Chalabieva, G.D. Geidarova, S.S. Alieva, Allylacetylenes and their derivatives as inhibitors of steel corrosion in sulphuric acid, Russian Journal of Applied Chemistry 79 (2006) 1829–1834.
[40] C. Fiaud, A. Harch, D. Mallouh, M. Tzinmann, The inhibition of iron corrosion by acetylenic alcohols in acid solutions at high temperature, Corrosion Science 35 (1993) 1437–1444.
[41] A. Rauschera, G. Kutsana, Z. Lukacsa, Studies on the mechanisms of corrosion inhibition by acetylenic compounds in hydrochloric acid solution, Corrosion Science 35 (1993) 1425–1430.
[42] S.P. Cardoso, J.A.C.P. Gomes, L.E.P. Borges, E. Hollauer, Predictive QSPR analysis of corrosion inhibitors for super 13% Cr steel in hydrochloric acid, Brazilian Journal of Chemical Engineering 24 (2007) 1250–1258.
[43] ASTM G 31-72 Standard Practice for Laboratory Immersion Corrosion Testing of Metals (re-approved 1995) 03.02 (1990).
[44] I.B. Obot, N.O. Obi-Egbedi, Adsorption properties and inhibition of mild steel corrosion in sulphuric acid solution by ketoconazole: experimental and theoretical investigation, Corrosion Science 52 (2010) 198–204.
[45] S. Deng, X. Li, H. Fu, Nitrotetrazolium blue chloride as a novel corrosion inhibitor of steel in sulphuric acid solution, Corrosion Science 52 (2010) 3840–3846.
[46] L.D. Paolinelli, T. Pérez, S.N. Simison, The effect of pre-corrosion and steel microstructure on inhibitor performance in CO_2 corrosion, Corrosion Science 50 (2008) 2456–2464.
[47] X. Wanga, H. Yang, F. Wang, An investigation of benzimidazole derivative as corrosion inhibitor for mild steel in different concentration HCl solutions, Corrosion Science 53 (2011) 113–121.
[48] A. Bouyanzer, B. Hammouti, L. Majidi, Pennyroyal oil from Mentha pulegium as corrosion inhibitor for steel in 1 M HCl, Material Letter 60 (2006) 2840–2843.
[49] K.C. Emregul, M. Hayvali, Studies on the effect of a newly synthesized Schiff base compound from phenazone and vanillin on the corrosion of steel in 2 M HCl, Corrosion Science 48 (2006) 797–812.
[50] M. Benabdellah, R. Souane, N. Cheriaa, R. Abidi, B. Hammouti, J. Vicens, Synthesis of calixarene derivatives and their anticorrosive effect on steel in 1 M HCl, Pigment and Resin Technology 36 (2007) 373–381.
[51] A. Popova, M. Christov, A. Zwetanova, Effects of the molecular structure on the inhibiter properties of azoles on mild steel corrosion in 1M hydrochloric acid, Corrosion Science 49 (2007) 2131–2143.
[52] A. Yildirim, M. Cetin, Synthesis and evaluation of new long alkyl side chain acetamide, isoxazolidine and isoxazoline derivatives as corrosion inhibitors, Corrosion Science 50 (2008) 155–165.
[53] M. Lebrini, M. Lagrenee, H. Vezin, M. Traisnel, F. Bentiss, Experimental and theoretical study for corrosion inhibition of mild steel in normal hydrochloric acid solution by some new macrocyclic polyether compounds, Corrosion Science 49 (2007) 2254–2269.
[54] J. Aljourani, K. Raeissi, M.A. Golozar, Benzimidazole and its derivatives as corrosion inhibitors for mild steel in 1 M HCl solution, Corrosion Science 51 (2009) 1836–1843.
[55] J.I. Bhat, V.D.P. Alva, Meclizine hydrochloride as a potential non-toxic corrosion inhibitor for mild steel in hydrochloric acid medium, Archives of Applied Science Research 3 (2011) 343–356.
[56] R. Touir, M. Cenoui, M. El Bakri, M. Ebn Touhami, Sodium gluconate as corrosion and scale inhibitor of ordinary steel in simulated cooling water, Corrosion Science 50 (2008) 1530–1537.
[57] E.A. Noor, A.H. Al-Moubaraki, Thermodynamic study of metal corrosion and inhibitor adsorption processes in mild steel/1-methyl-4[4′(-X)-styryl pyridinium iodides/hydrochloric acid systems, Materials Chemistry and Physics 110 (2008) 145–154.
[58] A. Asan, M. Kabasakaloglu, M. Isiklan, Z. Kilic, Corrosion inhibition of brass in presence of terdentate ligands in chloride solution, Corrosion Science 47 (2005) 1534–1544.
[59] Zh. Tao, Sh. Zhang, W. Li, B. Hou, Corrosion inhibition of mild steel in acidic solution by some oxo-triazole derivatives, Corrosion Science 51 (2009) 2588–2595.
[60] Y. Yan, W. Li, L. Cai, B. Hou, Electrochemical and quantum chemical study of purines as corrosion inhibitors for mild steel in 1 M HCl solution, Electrochimica Acta 53 (2008) 5953–5960.
[61] E. Cano, J.L. Polo, A. La Iglesia, J.M. Bastidas, A study on the adsorption of benzotriazole on copper in hydrochloric acid using the inflection point of the isotherm, Adsorption 10 (2004) 219–225.